

# Exponential Family Estimation via Adversarial Dynamics Embedding

\*Bo Dai<sup>1</sup>, \*Zhen Liu<sup>2</sup>, \*Hanjun Dai<sup>2</sup>, Niao He<sup>3</sup>,  
Arthur Gretton<sup>4</sup>, Le Song<sup>2</sup>, Dale Schuurmans<sup>1</sup>

<sup>1</sup>Google Brain, <sup>2</sup>Georgia Institute of Technology

<sup>3</sup>University of Illinois at Urbana Champaign, <sup>4</sup>University College London,

March 13, 2022

## Abstract

We present an efficient algorithm for maximum likelihood estimation (MLE) of the general exponential family, even in cases when the energy function is represented by a deep neural network. We consider the primal-dual view of the MLE for the kinetics augmented model, which naturally introduces an *adversarial* dual sampler. The sampler will be represented by a novel neural network architectures, *dynamics embeddings*, mimicking the dynamical-based samplers, *e.g.*, Hamiltonian Monte-Carlo and its variants. The dynamics embedding parametrization inherits the flexibility from HMC, and provides tractable entropy estimation of the augmented model. Meanwhile, it couples the adversarial dual samplers with the primal model, reducing memory and sample complexity. We further show that several existing estimators, including contrastive divergence (Hinton, 2002), score matching (Hyvärinen, 2005), pseudo-likelihood (Besag, 1975), noise-contrastive estimation (Gutmann and Hyvärinen, 2010), non-local contrastive objectives (Vickrey et al., 2010), and minimum probability flow (Sohl-Dickstein et al., 2011), can be recast as the special cases of the proposed method with different prefixed dual samplers. Finally, we empirically demonstrate the superiority of the proposed estimator against existing state-of-the-art methods on synthetic and real-world benchmarks.

## 1 Introduction

The exponential family is one of the most important classes of distributions in statistics and machine learning. It possesses a number of useful properties (Brown, 1986) and includes many commonly used distributions, and the notably powerful undirected graphical models (Wainwright and Jordan, 2008) and energy-based models (LeCun et al., 2006; Wu et al., 2018), *e.g.*, Markov random fields (Kinderman and Snell, 1980), conditional random fields (Lafferty et al., 2001), and language models (Mnih and Teh, 2012; Mnih and Kavukcuoglu, 2013). Despite the flexibility of the exponential family, a majority of models in this family are intractable due to the partition function having no known analytic form. This leads to difficulties in evaluating, sampling and learning of the model, which hinders its application in practice. In this paper, we try to provide an answer to the longstanding fundamental question:

*How to design a simple yet effective algorithm for estimating the exponential family distributions?*

There have been many attempts in the literature to answer this question. Since the maximum likelihood estimator (MLE) has already been well-studied with many desirable statistical properties, *e.g.*, consistency and asymptotic unbiasedness and normality (Brown, 1986), a major research direction lies in approximating the

---

\*indicates equal contribution. Email: bodai@google.com

MLE of the general exponential family. Contrastive divergence (CD) (Hinton, 2002) and its variants (Tieleman and Hinton, 2009; Du and Mordatch, 2019) are representative algorithms: rather than evaluating the gradient of the partition function, which also involves an intractable integral, CD exploits a stochastic gradient estimator with samples generated from a few Markov chain Monte Carlo (MCMC) steps. The major demerits of the CD algorithm and its variants are twofold: **i)**, it requires careful design of the transition kernel in MCMC, which is not a trivial task itself; more severely, **ii)**, the stochastic gradient is *biased*, which may lead to an inferior estimate.

Because of these difficulties with MLE, many other learning approaches have been introduced, including pseudo-likelihood (Besag, 1975), score matching (Hyvärinen, 2005), noise-contrastive estimation (Gutmann and Hyvärinen, 2010; Ceylan and Gutmann, 2018), and minimum probability flow (Sohl-Dickstein et al., 2011). Instead of approximating the MLE, these algorithms introduce alternative learning objectives that naturally sidestep the calculation of the partition function.

Pseudo-likelihood estimators (Besag, 1975) factorize the joint distribution by the product of conditional distributions, in which each factor is the distribution of a single random variable conditioned on the others. Even these conditional distributions can lack partition functions in analytic form for general exponential family distributions, however.

Score matching (Hyvärinen, 2005) instead minimizes the Fisher divergence between the empirical distribution and the model, in order to learn the parameters. The Fisher divergence involves only the derivatives of the potential function in the exponential family, and does not require computation of the partition function. Fisher score matching method requires the calculation of third order derivatives for the optimization procedure, however, which can be prohibitive for complex models (Kingma and LeCun, 2010).

Noise-contrastive estimation (Gutmann and Hyvärinen, 2010; Ceylan and Gutmann, 2018) recasts the problem as ratio estimation between the target distribution and a pre-defined auxiliary noise distribution. The ratio can then be estimated by logistic regression. The quality of the estimator and its statistical properties strongly rely on the choice of the auxiliary noise distribution, which needs to cover the support of the data, have an analytical expression, and be easy to sample. Such requirements are unlikely to be satisfied for many applications, especially in high dimensions.

Minimum probability flow (Sohl-Dickstein et al., 2011) leverages the observation that in an ideal case, the empirical distribution is the stationary distribution of the dynamics constructed from the optimal exponential family. MPF then estimates the model by matching these two distributions. Since the parameter in the model is implicitly represented through the dynamics, the objective also avoids the calculation of the partition function. While the idea behind the MPF is inspiring, the challenge remains to construct sampling dynamics for efficient learning.

In this paper, we introduce a novel algorithm, *Adversarial Dynamics Embedding (ADE)*, for learning and sampling from a maximum likelihood estimator, with a view to both computational and statistical efficiency. Our algorithm is largely motivated by the recent work of Dai et al. (2018a), who exploit a *primal-dual* view of the MLE that allows to bypass the computation of the intractable log-partition function. Such a view provides a natural objective for jointly learning both a sampler and a model, as an alternative to the expensive and biased MCMC steps in the CD algorithm. The parametrization of the dual sampler should be flexible to reduce the extra approximation error and density tractable for entropy computation in the objective. Dai et al. (2018a) consider the transport mapping for the dual distribution, leading to difficulty in entropy estimation, and thus requiring extra auxiliary distribution to be learned with additional computational and memory cost.

Inspired by the properties of Hamiltonian Monte-Carlo (HMC) (Neal et al., 2011), *i.e.*,

**i)**, HMC forms stationary distribution with *independent* potential and kinetic variables;

**ii)**, HMC can approximate the exponential family arbitrary closely,

we consider the *augmented distribution* with auxiliary kinetic variable as latent variable Section 3.1 and introduce *dynamics embedding* to parametrize the sampler by mimicking the sampling algorithms in Section 3.2. Due to the independence between potential and kinetic variables, the posterior of latent kinetic variable has explicit closed-form, eliminating the extra variational inference for latent kinetic variable. The dynamic embedding represents the dual samplers with tractable entropy via the primal model parameters, and thus

enrich the flexibility of sampler without introducing extra parameters. Finally, the *coupled* primal model and dual sampler will be learned *adversarially*, promoting the learning sample efficiency as described in Section 3.3.

We further demonstrate that the proposed estimator contains CD, pseudo-likelihood, score matching, non-local contrastive objectives, noise-contrastive estimation, and minimum probability flow as special cases with hand-designed dual samplers in Section 4. Our numerical experiments in Section 6 show that it also outperforms existing state-of-the-art estimators empirically.

## 2 Preliminaries

We provide a brief introduction to the technical background that is needed in the derivation of the new algorithm, including exponential family, dynamics-based MCMC sampler, and primal-dual view of MLE.

### 2.1 Exponential Family and Energy-based Model

The natural form of the exponential family over  $\Omega \subset \mathbb{R}^d$  is defined as

$$p_{f'}(x) = p_0(x) \exp(f'(x) - A(f')), \quad (1)$$

where  $A(f') := \log \int_{\Omega} \exp(f'(x)) p_0(x) dx$  and  $f'(x) = w^{\top} \phi_{\varpi}(x)$ . The sufficient statistic  $\phi_{\varpi}(\cdot) : \Omega \rightarrow \mathbb{R}^p$  can be general parametric model, *e.g.*, neural networks. The  $(w, \varpi)$  are the parameters that can be learned from observed data. The exponential family has been generalized to infinite dimensional case by setting  $f'$  belongs to some RKHSs (Sriperumbudur et al., 2017; Sutherland et al., 2017; Dai et al., 2018a). The energy-based model (LeCun et al., 2006) can be viewed as a special case of the exponential family by setting  $f'(x) = \phi_{\varpi}(x)$  with  $p = 1$ .

Traditionally, the  $p_0(x)$  is prefixed and covers the support  $\Omega$ , which is difficult in practical high-dimension problems. In this paper, we focus on learning  $f(x) = f(x) - \log p_0(x)$  with  $p_0(x)$  together, *i.e.*,

$$p_f(x) = \exp(f(x) - A(f)). \quad (2)$$

Given samples  $\mathcal{D} = [x_i]_{i=1}^N$  and denoting  $f \in \mathcal{F}$  as the valid parametrization family, the maximum log-likelihood estimation of the exponential family can be written as

$$\max_{f \in \mathcal{F}} L(f) := \widehat{\mathbb{E}}_{\mathcal{D}}[f(x)] - A(f), \quad (3)$$

which leads to the gradient as

$$\nabla_f L(f) = \widehat{\mathbb{E}}_{\mathcal{D}}[\nabla_f f(x)] - \mathbb{E}_{p_f(x)}[\nabla_f f(x)]. \quad (4)$$

Since  $A(f)$  and  $\mathbb{E}_{p_f(x)}[\nabla_f f(x)]$  are intractable, solving the MLE of general exponential family is extremely difficult.

### 2.2 Dynamics-based MCMC

The dynamics-based MCMC is a general and effective tool for inference. The basic idea of dynamics-based MCMC is to represent the target distribution as the solution to some (stochastic) differential equations. Therefore, samples of the target distribution can be obtained by simulating along the dynamics defined by the differential equations.

Hamiltonian Monte-Carlo (HMC) (Neal et al., 2011) is a representative algorithm in this category, which exploits the well-known Hamiltonian dynamics. Specifically, given a target distribution  $p_f(x) \propto \exp(f(x))$ , the Hamiltonian is defined as

$$\mathcal{H}(x, v) = -f(x) + k(v) \quad (5)$$

where  $k(v) = \frac{1}{2}v^\top v$  is the kinetic energy. The Hamiltonian dynamics generate  $(x, v)$  over time  $t$ , following

$$\left[ \frac{dx}{dt}, \frac{dv}{dt} \right] = [\partial_v \mathcal{H}(x, v), -\partial_x \mathcal{H}(x, v)] = [v, \nabla_x f(x)]. \quad (6)$$

Asymptotically as  $t \rightarrow \infty$ , the  $x$  follows the target distribution. In practical HMC, to reduce the error from discretization, an acceptance-rejection step can be introduced.

The finite-step dynamics-based MCMC sampler can be used for approximating  $\mathbb{E}_{p_f(x)} [\nabla f(x)]$  in (4), which leads to the CD algorithm (Hinton, 2002; Zhu and Mumford, 1998).

### 2.3 The Primal-Dual View of MLE

To address the intractability of the log-partition function  $A(f)$  in MLE (3), the Fenchel duality of  $A(f)$  has been exploited (Rockafellar, 1970; Wainwright and Jordan, 2008; Dai et al., 2018a), *i.e.*,

**Theorem 1 (Fenchel dual of log-partition, Proposition 5.1 (Wainwright and Jordan, 2008))** *Let  $H(q) := -\int_{\Omega} q(x) \log q(x) dx$ , we have:*

$$A(f) = \max_{q \in \mathcal{P}} \langle q(x), f(x) \rangle + H(q), \quad (7)$$

$$p_f(x) = \operatorname{argmax}_{q \in \mathcal{P}} \langle q(x), f(x) \rangle + H(q), \quad (8)$$

where  $\mathcal{P}$  denotes the space of distributions,  $\langle f, g \rangle = \int_{\Omega} f(x) g(x) dx$ .

Plugging the Fenchel dual of  $A(f)$  into the MLE (3), we achieve a saddle-point reformulation of  $L(f)$  as

$$\max_{f \in \mathcal{F}} \min_{q \in \mathcal{P}} \widehat{\mathbb{E}}_{\mathcal{D}}[f(x)] - \mathbb{E}_{q(x)}[f(x)] - H(q) \quad (9)$$

which bypasses the explicit computation of the partition function. Another by-product of the primal-dual view is that the dual distribution can be used in the inference stage, which usually requires executing relative expensive sampling algorithms in vanilla estimators.

The dual sampler plays a vital role in the primal-dual formulation of the MLE for exponential family estimation in (9). To achieve better performance, we have several principal requirements in parameterizing the dual distribution:

- i) the parametrization family needs to be *flexible* enough to diminish the error from solving the inner minimization problem;
- ii) the entropy of the parametrized dual distribution should be *tractable*.

Moreover, as shown in Theorem 1, the optimal dual sampler is totally decided by primal model  $f$ ,

- iii) the parametrized dual sampler should *explicitly incorporate* the primal model  $f$ .

Such dependence will reduce both the memory cost and sample complexity in the learning procedure. In the ideal case, the dual sampler is solely represented via  $f$ , and thus, no extra auxiliary component for dual sampler need to be learned.

A wide spectrum of techniques for distribution parametrization has been developed, such as the reparametrized latent variable models (Kingma and Welling, 2013; Rezende et al., 2014), transport mapping (Goodfellow et al., 2014), and normalizing flows (Rezende and Mohamed, 2015; Kingma et al., 2016; Dinh et al., 2016), *etc.*. However, none of these off-the-shelf parametrization satisfies the requirements about flexibility and density tractability simultaneously, not even to mention the dependency requirement. Specifically, the density value in transport mapping is intractable. On the other hand, the reparametrized trick restricts the distributions lie in known density form and the flow-based models rely on invertible operations, both limiting the expressive ability. Meanwhile, the reparametrized latent variable model requires extra variational posterior to be learned.

### 3 Adversarial Dynamics Embedding

In this section, we consider augmenting the original exponential family with kinetic variables. The primal-dual view of MLE for such new augmented model will naturally introduce an *adversarial* dual sampler with momentums as the latent variables that can be parametrized by *dynamic embedding*, satisfying all three requirements above without extra variational distribution introduced.

We start with the embeddings of classical Hamiltonian dynamics (Neal et al., 2011; Caterini et al., 2018) for dual distribution parametrization as an example, and discuss its generalized dynamics in latent space and the stochastic Langevin dynamics. This technique can be extended to other dynamics, each with its own advantages. We provide these extensions in Appendix B.

#### 3.1 Primal-Dual View of Augmented MLE

As we discussed, it is difficult to find a parametrization of  $q(x)$  in (9) satisfying all the three requirements simultaneously. Therefore, instead of directly working on (9) for original model, inspired with HMC, we consider the augmented exponential family  $p(x, v)$  with auxiliary momentum variable, *i.e.*,

$$\begin{aligned} p(x, v) &= \frac{\exp\left(f(x) - \frac{\lambda}{2} v^\top v\right)}{Z(f)}, \\ Z(f) &= \int \exp\left(f(x) - \frac{\lambda}{2} v^\top v\right) dx dv. \end{aligned} \quad (10)$$

The MLE of such model is

$$\begin{aligned} \max_f L(f) &:= \widehat{\mathbb{E}}_{x \sim \mathcal{D}} [\log p(x)] = \widehat{\mathbb{E}}_{x \sim \mathcal{D}} \left[ \log \int p(x, v) dv \right] \\ &= \widehat{\mathbb{E}}_{x \sim \mathcal{D}} \mathbb{E}_{p(v|x)} [\log p(x, v) - \log p(v|x)] \\ &= \widehat{\mathbb{E}}_{x \sim \mathcal{D}} \mathbb{E}_{p(v|x)} \left[ f(x) - \frac{\lambda}{2} v^\top v - \log p(v|x) \right] - Z(f) \end{aligned} \quad (11)$$

where the last equation comes from the definition of true posterior  $p(v|x)$ . By exploiting the independence between  $x$  and  $v$  in  $p(x, v)$  defined in (10), we have  $p(v|x) = \mathcal{N}\left(0, \lambda^{-\frac{1}{2}} I\right)$ . Applying the Fenchel dual to  $Z(f)$  of the augmented model (10), we derive the primal-dual view of (11), leading to the objective,

$$L(f) \propto \min_{q(x, v) \in \mathcal{P}} \widehat{\mathbb{E}}_{x \sim \mathcal{D}, p(v|x)} \left[ f(x) - \frac{\lambda}{2} v^\top v \right] - \mathbb{E}_{q(x, v)} \left[ f(x) - \frac{\lambda}{2} v^\top v - \log q(x, v) \right]. \quad (12)$$

**Remark (momentum as latent variable):** The  $q(x, v)$  in (12) contains latent variable  $v$ . One can exploit latent variable model for  $q(x) = \int q(x|v) q(v) dv$  in (9). However, the  $H(q)$  in (9) requires marginalization, which is intractable in general cases, and usually estimated via variational inference with extra posterior  $q(v|x)$  introduced. By directly considering the specifically designed augmented model, (12) eliminates such extra variational steps.

Similarly, one can introduce multiple momentums as the hierarchical latent variable augmented model, *i.e.*,

$$p\left(x, \{v^i\}_{i=1}^T\right) = \frac{\exp\left(f(x) - \sum_{i=1}^T \frac{\lambda_i}{2} \|v^i\|_2^2\right)}{Z(f)},$$

leading to the objective as

$$L(f) \propto \min_{q(x, \{v^i\}_{i=1}^T) \in \mathcal{P}} \widehat{\mathbb{E}}_{x \sim \mathcal{D}} [f(x)] - \mathbb{E}_{q(x, \{v^i\}_{i=1}^T)} \left[ f(x) - \sum_{i=1}^T \frac{\lambda_i}{2} \|v^i\|_2^2 - \log q\left(x, \{v^i\}_{i=1}^T\right) \right]. \quad (13)$$

### 3.2 Representing Dual Sampler via Primal Model

In this section, we introduce the Hamiltonian dynamic embedding representation of distributions for dual sampler, as well as its generalization and special instantiation.

The vanilla HMC is derived by discretizing the Hamiltonian dynamics defined in (6) with leapfrog integrator. Specifically, in a single time step, the sample  $(x, v)$  moves according to

$$(x', v') = \mathbf{L}_{f, \eta}(x, v) := \begin{pmatrix} v^{\frac{1}{2}} = v + \frac{\eta}{2} \nabla_x f(x) \\ x' = x + \eta v^{\frac{1}{2}} \\ v' = v^{\frac{1}{2}} + \frac{\eta}{2} \nabla_x f(x') \end{pmatrix}, \quad (14)$$

where  $\eta$  is defined as the leapfrog stepsize. Denote the one-step leapfrog as  $(x', v') = \mathbf{L}_{f, \eta}(x, v)$  and assume the  $(x^0, v^0) \sim q_\theta^0(x, v)$ , after  $T$  iterations, we obtain

$$(x^T, v^T) = \mathbf{L}_{f, \eta} \circ \mathbf{L}_{f, \eta} \circ \dots \circ \mathbf{L}_{f, \eta}(x^0, v^0), \quad (15)$$

which can be viewed as a neural network with special architecture. We term this *Hamiltonian (HMC) dynamics embedding*, by which the dual sampler is represented by the primal model, *i.e.*, the potential function  $f$ .

The flexibility of the HMC embedding for parameterizing the distribution actually comes from the nature of the dynamics-based samplers. In the limit the case, the proposed neural network (15) reduces to a gradient flow, whose stationary distribution is exactly the model distribution

$$p(x, v) = \operatorname{argmax}_{q(x, v) \in \mathcal{P}} \mathbb{E}_{q(x, v)} \left[ f(x) - \frac{\lambda}{2} v^\top v - \log q(x, v) \right].$$

Formally, the approximation ability of the HMC embedding can be justified,

**Theorem 2 (HMC embeddings as gradient flow)** *For a continuous time with infinitesimal stepsize  $\eta \rightarrow 0$ , the density of the particles  $(x^t, v^t)$ , denoted as  $q_t(x, v)$ , follows Fokker-Planck equation*

$$\frac{\partial q^t(x, v)}{\partial t} = \nabla \cdot (q^t(x, v) G \nabla \mathcal{H}(x, v)), \quad (16)$$

with  $G = \begin{bmatrix} 0 & \mathbf{I} \\ -\mathbf{I} & 0 \end{bmatrix}$ . Then  $q^t(x, v) \rightarrow p(x, v) \propto \exp(-\mathcal{H}(x, v))$  as  $t \rightarrow \infty$ .

Due to the space limit, the details of the proofs are postpone in Appendix A. As we can see, the neural network composed by HMC embedding can approximate well to exponential family distributions on continuous variables.

**Remark (Generalized HMC dynamics in latent space):** the leapfrog operation in the vanilla HMC is directly working in the original observation space, which is high-dimensional and noisy. We generalize the leapfrog update rule in latent space and form the new dynamics, *i.e.*,

$$v^{\frac{1}{2}} = v \odot \exp(S_v(\nabla_x f(x), x)) + \frac{\eta}{2} g_v(\nabla_x f(x), x), \quad (17)$$

$$x' = x \odot \exp\left(S_x\left(v^{\frac{1}{2}}\right)\right) + \eta g_x\left(v^{\frac{1}{2}}\right), \quad (18)$$

$$v' = v^{\frac{1}{2}} \odot \exp(S_v(\nabla_x f(x'), x')) + \frac{\eta}{2} g_v(\nabla_x f(x'), x'), \quad (19)$$

where  $\odot$  denotes the element-wise product. Specifically, the  $S_v(\nabla_x f(x), x)$  and  $S_x\left(v^{\frac{1}{2}}\right)$  rescales  $v$  and  $x$  coordinately. The  $g_v(\nabla_x f(x), x)$  can be understood as projecting the gradient information to the an essential latent space. Then, for updating  $x$ , the latent momentum is projected back to original space by  $g_x\left(v^{\frac{1}{2}}\right)$ .

With such generalized leapfrog updates, the dynamic system avoids operating the high-dimensional noisy input and become more efficient. We emphasize that the proposed generalized leapfrog parametrization (17) is different from the one used in Levy et al. (2017), which is inspired by the real-NVP flow (Dinh et al., 2016).

By embedding the generalized HMC (17), we have a flexible layer  $(x', v') = \mathbf{L}_{f, \eta, S, g}(x, v)$ . The  $(S_v, S_x, g_v, g_x)$  will be learned in addition to the stepsize. In fact, the vanilla HMC layer  $\mathbf{L}_{f, \eta, M}(x, v)$  is a special case of the  $\mathbf{L}_{f, \eta, S, g}(x, v)$  by setting  $(S_v, S_x)$  as zero and  $(g_v, g_f)$  as identity function.

**Remark (Stochastic Langevin dynamics):** we can recover the stochastic Langevin dynamics from leapfrog step by resampling momentum in every step. Specifically, the sample  $(x, \xi)$  moves according to

$$(x', v') = \mathbf{L}_{f, \eta}^{\xi}(x) := \begin{pmatrix} v' = \xi + \frac{\eta}{2} \nabla_x f(x) \\ x' = x + v' \end{pmatrix}, \quad (20)$$

where  $\xi \sim q_{\theta}(\xi)$ . As we can see, the stochastic Langevin dynamics resample  $\xi$  to replace the momentum in leapfrog (14), ignoring the gradient accumulation. After  $T$ -iteration, we obtain

$$(x^T, \{v^i\}_{i=1}^T) = \mathbf{L}_{f, \eta}^{\xi^{T-1}} \circ \mathbf{L}_{f, \eta}^{\xi^{T-2}} \circ \dots \circ \mathbf{L}_{f, \eta}^{\xi^0}(x^0), \quad (21)$$

as the derived neural network. Similarly, we can also generalize the stochastic Langevin updates  $\mathbf{L}_{f, \eta}^{\xi}$  by introducing  $g_v(\nabla_x f(x), x)$  and  $g_x(v')$  in corresponding positions.

On the other hand, the density value of the proposed neural network is also tractable, leading to tractable entropy estimation in (12) and (13). In particular, we have

**Theorem 3 (Density value evaluation)** *If  $(x^0, v^0) \sim q_{\theta}^0(x, v)$ , after  $T$  vanilla HMC steps (14), we have*

$$q^T(x^T, v^T) = q_{\theta}^0(x^0, v^0). \quad (22)$$

*For the  $(x^T, v^T)$  from the generalized leapfrog steps (17), we have*

$$q^T(x^T, v^T) = q_{\theta}^0(x^0, v^0) \prod_{t=1}^T (\Delta_x(x^t) \Delta_v(v^t)), \quad (23)$$

*where  $\Delta_x(x^t)$  and  $\Delta_v(v^t)$  denotes*

$$\begin{aligned} \Delta_x(x^t) &= |\det(\text{diag}(\exp(2S_v(\nabla_x f(x^t), x^t))))|, \\ \Delta_v(v^t) &= |\det(\text{diag}(\exp(S_x(v^{\frac{1}{2}}))))|. \end{aligned} \quad (24)$$

*For the  $(x^T, \{v^i\}_{i=1}^T)$  from the stochastic Langevin dynamics (20) with  $(x^0, \{\xi^i\}_{i=0}^{T-1}) \sim q_{\theta}^0(x, \xi) \prod_{i=0}^{T-1} q_{\theta_i}(\xi)$ , we have*

$$q^T(x^T, \{v^i\}_{i=1}^T) = q_{\theta}^0(x^0, \xi^0) \prod_{i=1}^{T-1} q_{\theta_i}(\xi^i). \quad (25)$$

The proof of Theorem 3 can be found in Appendix A.

As we can see, the proposed dynamics embedding satisfies all three requirements: it covers a flexible family of distributions with tractable density value, meanwhile, it couples the dual sampler with primal model, which leads to memory and sample efficient learning algorithm, as we will introduce in next section.

---

**Algorithm 1** MLE via Adversarial Dynamics Embedding (ADE)

---

```
1: Initialize  $\Theta_1$  randomly, set length of steps  $T$ .
2: for iteration  $k = 1, \dots, K$  do
3:   Sample mini-batch  $\{x_i\}_{i=1}^m$  from dataset  $\mathcal{D}$  and  $\{x_i^0, v_i^0\}_{i=1}^m$  from  $q_\theta^0(x, v)$ .
4:   for iteration  $t = 1, \dots, T$  do
5:     Compute  $(x^t, v^t) = \mathbf{L}(x^{t-1}, v^{t-1})$  for each pair of  $\{x_i^0, v_i^0\}_{i=1}^m$ .
6:   end for
7:   [Learning the sampler]  $\Theta_{k+1} = \Theta_k - \gamma_k \hat{\nabla}_\Theta \ell(f_k; \Theta_k)$ 
8:   [Estimating the exponential family]  $f_{k+1} = f_k + \gamma_k \hat{\nabla}_f \ell(f_k; \Theta_k)$ .
9: end for
```

---

### 3.3 Coupled Model and Sampler Learning

Plug the  $T$ -step Hamiltonian dynamics embedded parametrization (14) or (17) into the primal-dual MLE of the augmented model (12) and apply the density value evaluation in (22) and (23), respectively, we obtain our ultimate adversarial objective,

$$\max_{f \in \mathcal{F}} \min_{\Theta} \underbrace{\hat{\mathbb{E}}_{\mathcal{D}}[f] - \mathbb{E}_{(x^0, v^0) \sim q_\theta^0(x, v)} \left[ f(x^T) - \frac{\lambda}{2} \|v^T\|_2^2 \right] + \mathbb{E}_{(x^0, v^0) \sim q_\theta^0(x, v)} [\log q_\theta^0(x, v)]}_{\ell(f, \Theta)}. \quad (26)$$

Here  $\Theta$  denotes the learnable components in the dynamics embedding, *e.g.*, initialization  $q_\theta^0$ , the stepsize ( $\eta$ ) in the HMC/Langevin updates, and the adaptive part ( $S_v, S_x, g_v, g_x$ ) in the generalized HMC, which is learned adversarially. The parametrization of initial distribution is discussed in Appendix C. For the  $T$ -step stochastic Langevin dynamics embedded parametrization (20), we apply the density value (25) to (13), which leads to a similar saddle-point optimization with hierarchical momentums.

We can now use stochastic gradient descent to estimate  $f$  for the exponential families as well as the parameters in the dynamics embedding adversarially. Note that the generated sample  $(x_f^T, v_f^T)$  is a function of  $f$ , the gradient w.r.t.  $f$  should also take these variables into account as back-propagation through time (BPTT), *i.e.*,

$$\nabla_f \ell(f; \Theta) = \hat{\mathbb{E}}_{\mathcal{D}}[\nabla_f f(x)] - \mathbb{E}_{(x^0, v^0) \sim q_\theta^0(x, v)} [\nabla_f f(x^T)] - \mathbb{E}_{(x^0, v^0) \sim q_\theta^0(x, v)} [\nabla_x f(x^T) \nabla_f x^T + v^T \nabla_f v^T]. \quad (27)$$

We illustrate the MLE via HMC adversarial dynamics embedding (ADE) in Algorithm 1.

The same technique can be applied to other parametrization of dual sampler via alternative dynamics embeddings, as listed in Appendix B, leading to different architectures  $\mathbf{L}$  and the entropy term evaluations. Consider the dynamics embedding as an *adaptive* sampler that can be automatically learned w.r.t. different models and datasets, then, the updates for  $\Theta$  in can be understood as *learning to sample*.

## 4 Connections to Other Estimators

We establish the connections between the proposed estimator with existing approaches. In summary, the proposed algorithm is equipped with an adaptive sampler; while the existing algorithms can be recast as the special cases of our estimator with some hand-designed samplers, and thus, may lead to extra error and inferior solution.

### 4.1 Connection to Contrastive Divergence

The CD algorithm (Hinton, 2002) is a special case of the proposed algorithm. By Theorem 1, the optimal solution to the inner optimization is  $p(x, v) \propto \exp(-\mathcal{H}(x, v))$ . Applying Danskin's theorem (Bertsekas,



1995), the gradient of  $L(f)$  w.r.t.  $f$  is

$$\nabla_f L(f) = \widehat{\mathbb{E}}_{\mathcal{D}} [\nabla_f f(x)] - \mathbb{E}_{p_f(x)} [\nabla_f f(x)]. \quad (28)$$

To estimate the integral  $\mathbb{E}_{p_f} [\nabla_f f(x)]$ , the CD algorithm approximates the negative term in (28) stochastically with a finite MCMC step away from empirical data.

In the proposed dual sampler, by setting  $p_{\theta}^0(x)$  to be the empirical distribution and eliminating the sampling learning, the dynamic embedding will collapse to CD with  $T$ -HMC steps if we remove gradient through the sampler, *i.e.*, ignoring the third term in (27). Similarly, the persistent CD (PCD) (Tieleman, 2008) and recent ensemble CD (Du and Mordatch, 2019) can also be recast as special cases by setting the negative sampler to be MCMC with initial samples from previous model and ensemble of MCMC samplers, respectively.

From this perspective, the CD and PCD algorithms induce errors not only from the sampler, but also from the gradient back-propagation truncation. The proposed algorithm escapes these sources of bias by learning to sample, and by adopting true gradients, respectively. Therefore, the proposed estimator is expected to achieve better performance than CD as demonstrated in the empirical experiments Section 6.2.

## 4.2 Connection to Score Matching

The score matching (Hyvärinen, 2005) estimates the exponential family by minimizing the Fisher divergence, leading to optimization,

$$L_{SM}(f) := -\mathbb{E}_{\mathcal{D}} \left[ \sum_{i=1}^d \left( \frac{1}{2} (\partial_i f(x))^2 \right) + \partial_i^2 f(x) \right]. \quad (29)$$

As explained in Hyvärinen (2007), the objective (29) can be derived as the 2nd-order Taylor approximation of the MLE with 1-step Langevin Monte Carlo as the dual sampler. Specifically, the Langevin Monte Carlo generates samples via

$$x' = x + \frac{\eta}{2} \nabla_x f(x) + \sqrt{\eta} \xi, \quad \xi \sim \mathcal{N}(0, I),$$

then, a simple Taylor expansion gives

$$\log p_f(x') = \log p_f(x) + \sum_{i=1}^d \partial_i f(x') (\partial_i f(x) + \sqrt{\eta} \xi_i) + \frac{\eta}{2} \sum_{i,j=1}^d \xi_i \xi_j \partial_{ij}^2 f(x') + o(\eta).$$

Plug such into the negative expectation in  $L(f)$ , leading to

$$L(f) \approx \widehat{\mathbb{E}}_{\mathcal{D}} [\log p_f(x) - \mathbb{E}_{x'|x} [\log p_f(x')]] \approx -\mathbb{E}_{\mathcal{D}} \left[ \sum_{i=1}^d \left( \frac{1}{2} (\partial_i f(x))^2 \right) + \partial_i^2 f(x) \right],$$

which is exactly the  $L_{SM}(f)$  defined in (29).

Therefore, the score matching can be viewed as applying Taylor expansion approximation with fixed 1-step Langevin sampler in our framework, which is compared in Section 6.1.

## 4.3 Connection to Pseudo-Likelihood and Conditional Composite Likelihood

The pseudo-likelihood estimation (Besag, 1975) is a special case of the proposed algorithm by restricting the parametrization of the dual distribution. Specifically, denote the  $p_f(x_i|x_{-i}) = \frac{\exp(f(x_i, x_{-i}))}{Z(x_{-i})}$  with  $Z(x_{-i}) := \int \exp(f(x_i, x_{-i})) dx_i$ , instead of directly maximizing likelihood, the pseudo-likelihood estimator is maximizing

$$L_{PL}(f) := \widehat{\mathbb{E}}_{\mathcal{D}} \left[ \sum_{i=1}^d \log p_f(x_i|x_{-i}) \right]. \quad (30)$$

Then, the  $f$  is updated by the following the gradient of  $L_{pl}(f)$ , *i.e.*,

$$\nabla_f L_{PL}(f) \propto \widehat{\mathbb{E}}_{\mathcal{D}} [\nabla_f f(x)] - \mathbb{E}_{i \sim \mathcal{U}(d)} \widehat{\mathbb{E}}_{x_{-i}} \mathbb{E}_{p_f(x_i|x_{-i})} [\nabla_f f(x_i, x_{-i})].$$

The pseudo-likelihood estimator can be recast as a special case of the proposed framework if we fix the dual sampler as **i)**, sample  $i \in \{1, \dots, d\}$  uniformly; **ii)**, sample  $x \sim \mathcal{D}$  and mask  $x_i$ ; **iii)**, sample  $x_i \sim p_f(x_i|x_{-1})$  and compose  $(x_i, x_{-i})$ .

The conditional composite likelihood (Lindsay, 1988) is a generalization of pseudo-likelihood by maximizing

$$L_{CL}(f) := \widehat{\mathbb{E}}_{\mathcal{D}} \left[ \sum_{A_i=1}^m \log p_f(x_{A_i}|x_{-A_i}) \right], \quad (31)$$

where  $\{A_i\}_{i=1}^m = d$  and  $A_i \cap A_j = \emptyset$ . Similarly, the composite likelihood is updating with prefixed conditional block sampler for negative sampling.

Same as CD, the prefixed sampler and the biased gradient in pseudo-likelihood and composite likelihood estimator will induce extra errors and lead to inferior solution. Moreover, the pseudo-likelihood may not applicable to the general exponential family with continuous variables, whose conditional distribution is also intractable.

#### 4.4 Connection to Non-local Contrastive Objectives

The non-local contrastive estimator (Vickrey et al., 2010) is obtained by maximizing

$$L_{NCO}(f) := \widehat{\mathbb{E}}_{\mathcal{D}} \left[ \sum_{i=1}^m w(x, S_i) (f(x) - \log Z_i(f)) \right], \quad (32)$$

where  $[S_i]_{i=1}^m$  denotes some prefixed partition of  $\Omega$ ,  $Z_i(f) = \int_{x \in S_i} \exp(f(x)) dx$ , and  $w(x, S_i) = P(x \in S_i|x)$  with  $\sum_{i=1}^m w(x, S_i) = 1$ . The objective (32) leads to the update direction as

$$\nabla_f L_{NCO}(f) = \widehat{\mathbb{E}}_{\mathcal{D}} [\nabla_f f(x)] - \mathbb{E}_{q_f(x)} [\nabla_f f], \quad (33)$$

where  $q_f(x) = \sum_{i=1}^m \int p_{(f,i)}(x) w(x', S_i) p_{\mathcal{D}}(x') dx$  with  $p_{\mathcal{D}}$  as the empirical distribution and  $p_{(f,i)}(x) = \frac{\exp(f(x))}{Z_i(f)}$ ,  $x \in S_i$ . Therefore, the non-local contrastive objective is a special case of the proposed framework with the dual sampler as **i)**, sample  $x'$  uniformly from  $\mathcal{D}$ ; **ii)**, sample  $S_i$  conditional on  $x'$  according to  $w(x, S_i)$ ; **iii)**, sample  $x_i \sim p_{(f,i)}(x)$  within  $S_i$ . Such negative sampling method is also not applicable to the general exponential family with continuous variables.

#### 4.5 Connection to Minimum Probability Flow

In the continuous state model, the minimum probability flow (Sohl-Dickstein et al., 2011) estimates the exponential family by maximizing

$$L_{MPF}(f) := -\widehat{\mathbb{E}}_{x \sim \mathcal{D}} \mathbb{E}_{x' \sim \mathcal{T}_f(x'|x)} \left[ \exp \left( \frac{1}{2} (f(x') - f(x)) \right) \right],$$

where  $\mathcal{T}_f$  is a *hand-designed* symmetric transition kernel based on the potential function  $f(x)$ , *e.g.*, Hamiltonian or Langevin simulation. Then, the MPF update direction can be rewritten as

$$\widehat{\mathbb{E}}_{x \sim \mathcal{D}} \mathbb{E}_{x' \sim \Gamma(x'|x)} [\nabla_f f(x) - \nabla_f f(x') - \nabla_x f(x') \nabla_f x']. \quad (34)$$

where  $\Gamma(x'|x) := \mathcal{T}_f(x'|x) \exp \left( \frac{1}{2} (f(x') - f(x)) \right)$ . The probability flow operator  $\Gamma(x'|x)$  actually defines a Markov chain sampler that achieves the following balance equation,

$$\Gamma(x'|x) p_f(x) = \Gamma(x|x') p_f(x').$$

Similar to CD and score matching, the MPF exploits the 1-step MCMC. Moreover, the gradient in MPF also considers the effects in sampler as the third term in (34). Therefore, the MPF can be recast as a special case of our algorithm with the prefixed dual sampler as  $x \sim \mathcal{D}$  and  $x' \sim \Gamma(x'|x)$ .

## 4.6 Connection to Noise-Contrastive Estimator

Instead of directly estimating the  $f$  in the exponential family, Gutmann and Hyvärinen (2010) propose the noise-contrastive estimation (NCE) for the density ratio between the exponential family and some user defined reference distribution  $p_n(x)$ , from which the parameter  $f$  can be reconstructed. Specifically, the NCE considers an alternative representation of exponential family distribution as  $p_f(x) = \exp(f(x))$ , which explicitly enforces  $\int \exp(f(x)) dx = 1$ . The NCE is obtained by maximizing

$$L_{NCE}(f) := \hat{\mathbb{E}}_{\mathcal{D}} [\log h(x)] + \mathbb{E}_{p_n(x)} [\log (1 - h(x))], \quad (35)$$

where  $h(x) = \frac{\exp(f(x))}{\exp(f(x)) + p_n(x)}$ . Then, we have the gradient of  $L_{NCE}(f)$  as

$$\nabla_f L_{NCE}(f) = \hat{\mathbb{E}}_{\mathcal{D}} [\nabla_f f(x)] - \mathbb{E}_{\frac{1}{2}p_{\mathcal{D}} + \frac{1}{2}p_n} [h(x) \nabla_f f(x)]. \quad (36)$$

The negative sampler in the (36) can be understood as an approximate importance sampling algorithm where the proposal is  $\frac{1}{2}p_{\mathcal{D}} + \frac{1}{2}p_n$  and the reweighting part is  $h(x)$ . As the  $\exp(f)$  approaching  $p_{\mathcal{D}}$ , the  $h(x)$  will approach the true ratio  $\frac{\exp(f(x))}{p_{\mathcal{D}} + p_n(x)}$ , and thus, the negative samples will converge to true model samples.

The NCE can be understood as learning an important sampler. However, the performance of NCE highly relies on the quality  $h(x)$ , *i.e.*, the choice of  $p_n(x)$ . It is required to cover the support of  $p_{\mathcal{D}}(x)$ , which is non-trivial in practical high-dimensional applications.

## 5 Related Work

The parametrization of the dual sampler should be both flexible enough and density tractable to achieve better performance. Pioneering works are limited in either one aspect or other. Kim and Bengio (2016) parameterize the sampler via a deep directed graphical model, whose approximation ability is limited to known distributions. Meanwhile, they fit  $q$  by minimizing the reverse  $KL$ -divergence to avoid the entropy calculation, leading to unclear relationship to MLE. Due to the difficulty of the entropy term for general transport mapping parametrization, a variety of approximate surrogates have been proposed to relax the density value tractability requirement. Liu and Wang (2017) learn the sampler  $q$  to mimic the Stein variational gradient descent sampling procedure; Dai et al. (2017) propose algorithms relying on either a heuristic approximation or a upper bound of the entropy, with extra auxiliary component introduced to be learned; Dai et al. (2018a) apply a second Fenchel dual representation to reformulate the entropy term, at the cost of introducing another auxiliary function to be estimated. Meanwhile, the second Fenchel duality parametrization relies on a proposal distribution with the same support for numerical stability, which is impractical for high-dimensional data. In contrast to these existing methods, the proposed dynamics embedding achieves both flexibility and tractability of entropy estimation with less independent auxiliary parameters introduced. Moreover, the dynamics embedding avoids the design of proposal, which is naturally suitable for high-dimension data.

One of our major contributions is learning a sampling strategy for the exponential family estimation through the primal-dual view of MLE. The proposed algorithm shares some similarities with recent advances in meta learning for sampling (Levy et al., 2017; Feng et al., 2017; Song et al., 2017; Gong et al., 2018), in which the sampler is parametrized via neural network and will be learned through certain objectives. However, we emphasize that the most significant difference lies in the ultimate goals: we focus on exponential family *model estimation* and the learned sampler is only introduced to *assist* with this objective. By contrast, the learning to sample techniques are targeting on learning a *fixed* model that is already given. This fundamentally distinguishes the proposed ADE from methods that only learns samplers, leading to totally different learning criterion and algorithm updates, *i.e.*, the primal model will be learned back through the learned sampler, from which perspective the proposed algorithm can be understood as meta<sup>2</sup>-learning.

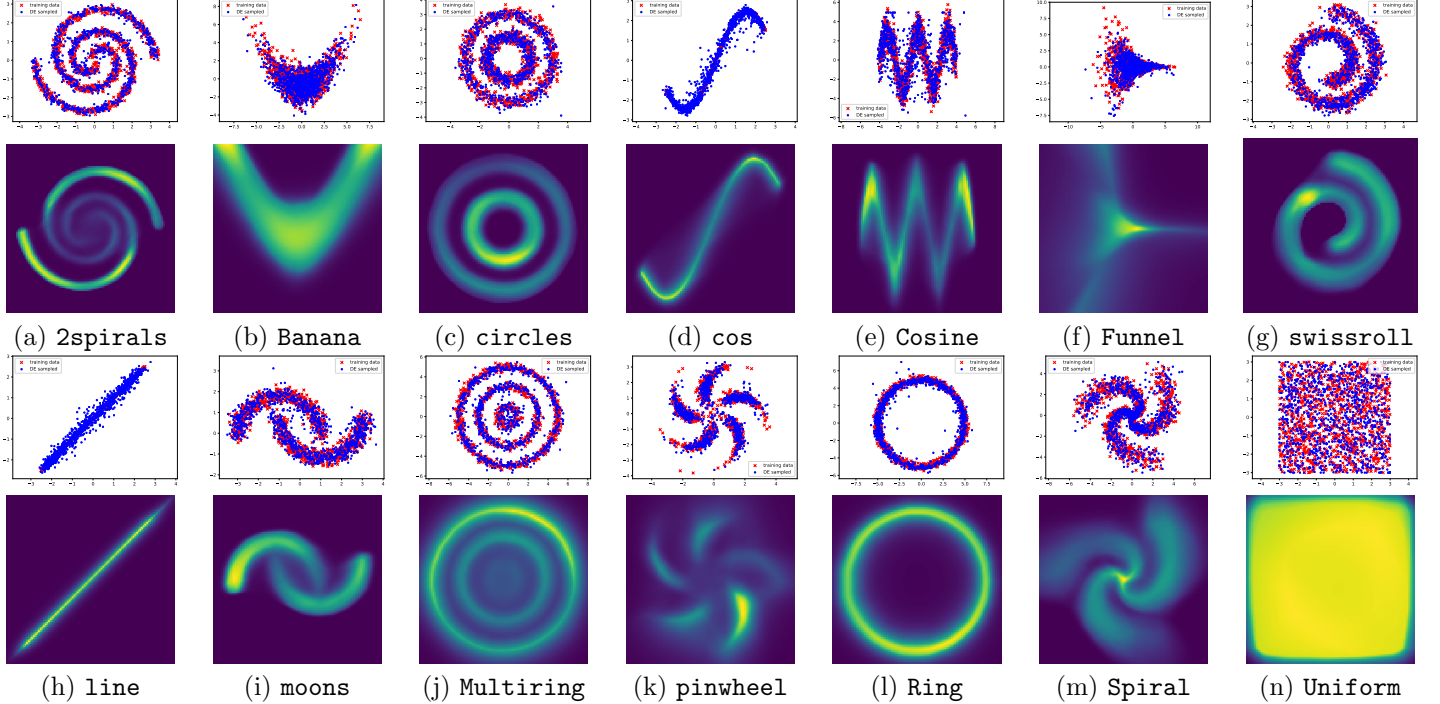


Figure 1: Learned samplers in odd row and potential function  $f$  in even row from different synthetic datasets.

## 6 Experiments

### 6.1 Synthetic experiments

We parametrize the potential function  $f$  with fully connected multi-layer perceptron with 3 hidden layers. Each hidden layer has 128 hidden units. We use ReLU to do the nonlinear activation in each hidden layer. For baseline methods, we compare with score matching (SM) estimator (Hyvärinen, 2005) and primal-dual MLE with the normalizing flow (Rezende and Mohamed, 2015) parametrized dual sampler (NF). Note that although the normalizing flow can be used to perform maximum likelihood estimation (MLE) to fit the data (Rezende and Mohamed, 2015), here the flow is asked to help train the exponential model  $f$ . Using normalizing flow to learn the exponential family model can be viewed as the special case of our method, which has only  $q_\theta^0$  parameterized as flow, but no HMC dynamics is involved. Thus this is also served as one ablation study for the proposed ADE.

For our method, we use normalizing flow as the initial proposal distribution  $x^0 \sim q_\theta^0(x)$ . Then we perform several steps of stochastic Langevin operation to get the final samples  $x^T$ .  $\{\xi^i\}_{i=0}^{T-1} \sim \mathcal{N}(0, I)$  is the distribution for sampling momentum. We clip the norm of  $\nabla_x f$  when updating  $v$ , and clip  $v$  when updating  $x$ . The coefficient  $\lambda$  in (26) is tuned in  $\{0.1, 0.5, 1\}$ . For the NF baseline, we tune the number of layers in  $\{10, 15, 20\}$ . For our ADE, we fix the number of normalizing flow layers to be 10, and then perform at most 10 steps of dynamics updates. So finally, the number of steps for sampling is comparable, while the ADE maintains less memory cost.

In this section, we compare the proposed ADE with other baseline methods on several synthetic datasets. For visualization purpose, all the samples are in  $\mathbb{R}^2$  space. The dataset generators are collect from several open-source projects<sup>1 2</sup>. During training, we use this generator to generate the data from the true distribution on the fly. To get a quantitative comparison, we also generate 1,000 data samples for held-out evaluation.

<sup>1</sup><https://github.com/rtgichen/ffjord>

<sup>2</sup><https://github.com/kevin-w-li/deep-kexpfam>

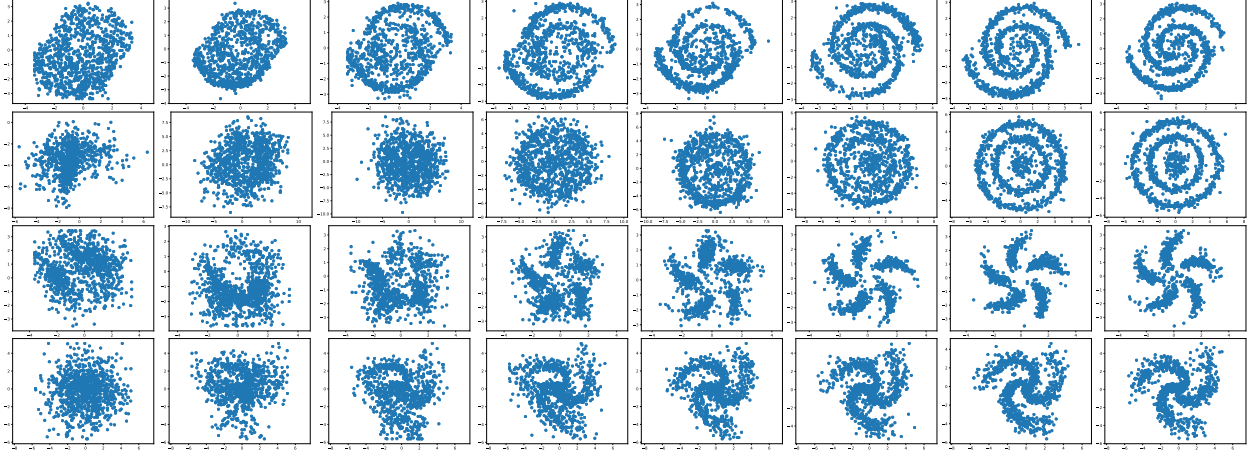


Figure 2: Convergence behavior of sampler on **2spirals**, **Multiring**, **pinwheel**, **Spiral** synthetic datasets.

In Figure 1, we visualize the learned distribution using both the learned dual sampler and also the exponential model  $\exp(c \cdot f)$ , where  $c$  is a constant that is tuned within  $[0.01, 10]$ . Overall one can see the sampler almost perfectly recover the distribution, and the learned  $f$  almost captures the landscape of the distribution. We also visualize the convergence behavior in Figure 2. We can see the samples are converging to the true data distribution smoothly. As the learned sampler depends on the  $f$ , so this figure also suggests the nice convergence behavior of  $f$  indirectly.

The quantitative comparison of the sampler is illustrated in Table 1. For NF and ADE, we use 1,000 samples from their sampler to calculate MMD with gaussian kernel. The kernel bandwidth is chosen using median trick (Dai et al., 2016). For SM, since there is no such sampler available, we directly use vanilla HMC to get sample from the learned model  $f$ , and use them to estimate MMD. From the table we can see, our approach gets the best MMD in all cases. This demonstrates the effectiveness of dynamics embedding, as comparing to only using the normalizing flow model.

Table 1: Quantitative comparison on synthetic data using maximum mean discrepancy ( $\text{MMD} \times 1e^{-3}$ ).

Dataset	SM	NF	ADE
<b>2spirals</b>	5.09	0.69	<b>-0.76</b>
<b>Banana</b>	8.10	0.88	<b>-1.13</b>
<b>circles</b>	4.90	0.76	<b>-1.30</b>
<b>cos</b>	10.36	0.91	<b>-0.58</b>
<b>Cosine</b>	8.34	2.15	<b>-1.00</b>
<b>Funnel</b>	13.07	-0.92	<b>-1.02</b>
<b>swissroll</b>	19.93	1.97	<b>-0.97</b>
<b>line</b>	10.28	0.39	<b>-0.53</b>
<b>moons</b>	41.34	0.80	<b>-1.04</b>
<b>Multiring</b>	2.01	0.30	<b>-1.05</b>
<b>pinwheel</b>	18.41	3.01	<b>-0.83</b>
<b>Ring</b>	9.22	161.89	<b>-1.38</b>
<b>Spiral</b>	9.48	5.96	<b>-0.62</b>
<b>Uniform</b>	5.88	0.00	<b>-1.08</b>

## 6.2 Real-world Image Datasets

To further verify that the proposed adversarial dynamics embedding can learn complicated exponential family and the corresponding sampler well for real-world images, we trained models on **MNIST** and **CIFAR-10** dataset. For both datasets, we use the CNN architecture for discriminator as used in Miyato et al. (2018), and spectral normalization is added to all discriminator layers. Specifically, for the discriminator in **CIFAR-10** experiments, we replace all downsampling operations by average pooling, as in Du and Mordatch (2019). The detailed architectures are shown in Appendix C.3.

We parametrize the initial distribution  $p_0(x, v)$  with neural nets as deep Gaussian latent variable model (Deep LVM) specified in Appendix C. After several HMC steps on this initial distribution, instead of clipping the images, we pass the sample to tanh function to obtain the final sampled images.

We used the standard spectral normalization on the discriminator to stabilize the training process, and

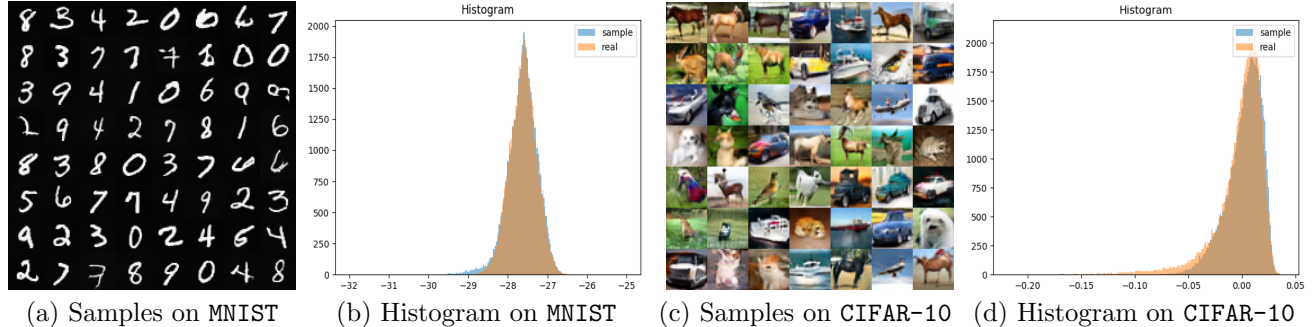


Figure 3: The generated images on MNIST and CIFAR-10 and the comparison between energies of generated samples and real images. The blue histogram illustrates the distribution of  $f(x)$  on generated samples, and the orange histogram is generated by  $f(x)$  on testing samples. As we can see, the learned potential function  $f(x)$  matches the empirical dataset well.

Adam with learning rate  $10^{-4}$  to optimize our model. We trained the models with 200000 iterations with batch size being 64. The step sizes for our HMC sampler are independently learned for all HMC dimensions but shared among all time steps, and the values are all initialized to  $3e - 1$ . We set the number of HMC steps to 15. The coefficient of the entropy regularization term is set to  $10^{-5}$  and that of the  $L_2$  regularization on the momentum vector in the last HMC step is set to  $10^{-2}$ .

Model	Inception Score
WGAN-GP (Gulrajani et al., 2017)	6.50
Spectral GAN (Miyato et al., 2018)	7.42
Langevin PCD (Du and Mordatch, 2019)	6.02
Langevin PCD (10 ensemble) (Du and Mordatch, 2019)	6.78
ADE: Deep LVM init w/o HMC	6.51
ADE: Deep LVM init w/ HMC	<b>7.43</b>

Table 2: Inception scores of different models on CIFAR-10 (unconditional).

We report the inception scores in Table 2. For our ADE, we trained two models with Deep LVM as the initial dual sampler, one with HMC samplers and one without that. We observed that the HMC sampler greatly improves the performance of the samples generated by initial Deep LVM along and enables the generator to be comparable with Spectral GAN. Moreover, we note that the initial Deep LVM helps sample generation, compared to the Langevin PCD models reported in (Du and Mordatch, 2019).

We show some samples of generated images in Figure 3(a) and (c). More sampled images can be found in Appendix D. In addition, we also plot the potential distribution (unnormalized) of generated samples and that of the real images on MNIST and CIFAR-10 (using 1000 data points for each) in Figure 3(b) and (d). The distributions of energies of both generated images and real iamges mostly overlap with each other, showing that the discriminators learn the desirable distributions. Also, with simple importance sampling and proposal distribution being uniform distribution on  $[-1, 1]^{n_d}$  ( $n_d$  is the dimension of images), the log likelihood (in nats) on CIFAR-10 is estimated to be around 2100.

## 7 Conclusion

We proposed a novel method to efficiently construct maximum likelihood estimator (MLE) for general exponential families. Specifically, by utilizing the nice properties of primal-dual formulation of the MLE

of the augmented exponential family distribution with kinetic variables, we incorporate dynamics-based distribution parametrization for dual sampler into the estimation process in a fully differentiable way. Such coupling of the primal model and the dual sampler benefits each other, and thus, achieving both better model estimation and efficient inference at the same time. Our empirical results on both synthetic and real data validate the feasibility of our proposed dynamics embedding. In future work, we will extend this method to other graphical model learning problems.

## Acknowledgements

NH is supported in part by NSF-CRII-1755829, NSF-CMMI-1761699, and NCSA Faculty Fellowship. LS is supported in part by NSF IIS-1218749, NIH BIGDATA 1R01GM108341, NSF CAREER IIS-1350983, NSF IIS-1639792 EAGER, NSF IIS-1841351 EAGER, NSF CCF-1836822, NSF CNS-1704701, ONR N00014-15-1-2340, Intel ISTC, NVIDIA, Amazon AWS, Siemens and Google Cloud.

## References

- D. P. Bertsekas. *Nonlinear Programming*. Athena Scientific, Belmont, MA, 1995.
- J. Besag. Statistical analysis of non-lattice data. *The Statistician*, 24:179–195, 1975.
- Christos Boutsidis, Petros Drineas, Prabhanjan Kambadur, Eugenia-Maria Kontopoulou, and Anastasios Zouzias. A randomized algorithm for approximating the log determinant of a symmetric positive definite matrix. *Linear Algebra and its Applications*, 533:95–117, 2017.
- Lawrence D. Brown. *Fundamentals of Statistical Exponential Families*, volume 9 of *Lecture notes-monograph series*. Institute of Mathematical Statistics, Hayward, Calif, 1986.
- Anthony L Caterini, Arnaud Doucet, and Dino Sejdinovic. Hamiltonian variational auto-encoder. *arXiv preprint arXiv:1805.11328*, 2018.
- Ciwan Ceylan and Michael U Gutmann. Conditional noise-contrastive estimation of unnormalised models. *arXiv preprint arXiv:1806.03664*, 2018.
- Bo Dai, Niao He, Hanjun Dai, and Le Song. Provable bayesian inference via particle mirror descent. In *Proceedings of the 19th International Conference on Artificial Intelligence and Statistics*, pages 985–994, 2016.
- Bo Dai, Hanjun Dai, Arthur Gretton, Le Song, Dale Schuurmans, and Niao He. Kernel exponential family estimation via doubly dual embedding. 2018a. URL <http://arxiv.org/abs/1811.02228>.
- Bo Dai, Hanjun Dai, Niao He, Weiyang Liu, Zhen Liu, Jianshu Chen, Lin Xiao Xiao, and Le Song. Coupled variational bayes via optimization embedding. In *NIPS*, 2018b.
- Zihang Dai, Amjad Almahairi, Philip Bachman, Eduard Hovy, and Aaron Courville. Calibrating energy-based generative adversarial networks. *arXiv preprint arXiv:1702.01691*, 2017.
- Laurent Dinh, Jascha Sohl-Dickstein, and Samy Bengio. Density estimation using real nvp. *arXiv preprint arXiv:1605.08803*, 2016.
- Yilun Du and Igor Mordatch. Implicit generation and generalization in energy-based models. *arXiv preprint arXiv:1903.08689*, 2019.
- Yihao Feng, Dilin Wang, and Qiang Liu. Learning to draw samples with amortized stein variational gradient descent. *arXiv preprint arXiv:1707.06626*, 2017.

- Wenbo Gong, Yingzhen Li, and José Miguel Hernández-Lobato. Meta-learning for stochastic gradient mcmc. *arXiv preprint arXiv:1806.04522*, 2018.
- Ian Goodfellow, Jean Pouget-Abadie, Mehdi Mirza, Bing Xu, David Warde-Farley, Sherjil Ozair, Aaron Courville, and Yoshua Bengio. Generative adversarial nets. In *Advances in Neural Information Processing Systems*, pages 2672–2680, 2014.
- Will Grathwohl, Ricky TQ Chen, Jesse Bettencourt, Ilya Sutskever, and David Duvenaud. Ffjord: Free-form continuous dynamics for scalable reversible generative models. *arXiv preprint arXiv:1810.01367*, 2018.
- Ishaan Gulrajani, Faruk Ahmed, Martin Arjovsky, Vincent Dumoulin, and Aaron C Courville. Improved training of wasserstein gans. In *Advances in Neural Information Processing Systems*, pages 5767–5777, 2017.
- Michael Gutmann and Aapo Hyvärinen. Noise-contrastive estimation: A new estimation principle for unnormalized statistical models. In *Proceedings of the Thirteenth International Conference on Artificial Intelligence and Statistics*, pages 297–304, 2010.
- Insu Han, Dmitry Malioutov, and Jinwoo Shin. Large-scale log-determinant computation through stochastic chebyshev expansions. In *International Conference on Machine Learning*, pages 908–917, 2015.
- Geoffrey E. Hinton. Training products of experts by minimizing contrastive divergence. *Neural Computation*, 14(8):1771–1800, 2002.
- A. Hyvärinen. Estimation of non-normalized statistical models using score matching. *Journal of Machine Learning Research*, 6:695–709, 2005.
- Aapo Hyvärinen. Some extensions of score matching. *Computational statistics & data analysis*, 51(5): 2499–2512, 2007.
- Taesup Kim and Yoshua Bengio. Deep directed generative models with energy-based probability estimation. *arXiv preprint arXiv:1606.03439*, 2016.
- R. Kinderman and J. L. Snell. *Markov Random Fields and their applications*. Amer. Math. Soc., Providence, RI, 1980.
- Diederik P Kingma and Prafulla Dhariwal. Glow: Generative flow with invertible 1x1 convolutions. *arXiv preprint arXiv:1807.03039*, 2018.
- Diederik P Kingma and Yann LeCun. Regularized estimation of image statistics by score matching. In *NIPS*, 2010.
- Diederik P Kingma and Max Welling. Auto-encoding variational bayes. *arXiv preprint arXiv:1312.6114*, 2013.
- Diederik P Kingma, Tim Salimans, Rafal Jozefowicz, Xi Chen, Ilya Sutskever, and Max Welling. Improved variational inference with inverse autoregressive flow. In *Advances in Neural Information Processing Systems*, pages 4743–4751, 2016.
- J. D. Lafferty, A. McCallum, and F. Pereira. Conditional random fields: Probabilistic modeling for segmenting and labeling sequence data. In *Proceedings of International Conference on Machine Learning*, volume 18, pages 282–289, San Francisco, CA, 2001. Morgan Kaufmann.
- Yann LeCun, Sumit Chopra, Raia Hadsell, M Ranzato, and F Huang. A tutorial on energy-based learning. *Predicting structured data*, 1(0), 2006.
- Daniel Levy, Matthew D Hoffman, and Jascha Sohl-Dickstein. Generalizing hamiltonian monte carlo with neural networks. *arXiv preprint arXiv:1711.09268*, 2017.



- B. G. Lindsay. Composite likelihood methods. *Contemporary Mathematics*, 80(1):221–239, 1988.
- Qiang Liu and Dilin Wang. Learning deep energy models: Contrastive divergence vs. amortized mle. *arXiv preprint arXiv:1707.00797*, 2017.
- Takeru Miyato, Toshiki Kataoka, Masanori Koyama, and Yuichi Yoshida. Spectral normalization for generative adversarial networks. *arXiv preprint arXiv:1802.05957*, 2018.
- Andriy Mnih and Koray Kavukcuoglu. Learning word embeddings efficiently with noise-contrastive estimation. In *Advances in Neural Information Processing Systems*, pages 2265–2273, 2013.
- Andriy Mnih and Yee Whye Teh. A fast and simple algorithm for training neural probabilistic language models. *arXiv preprint arXiv:1206.6426*, 2012.
- Radford M Neal et al. Mcmc using hamiltonian dynamics. *Handbook of Markov Chain Monte Carlo*, 2(11), 2011.
- Danilo J Rezende, Shakir Mohamed, and Daan Wierstra. Stochastic backpropagation and approximate inference in deep generative models. In *Proceedings of the 31st International Conference on Machine Learning (ICML-14)*, pages 1278–1286, 2014.
- Danilo Jimenez Rezende and Shakir Mohamed. Variational inference with normalizing flows. *arXiv preprint arXiv:1505.05770*, 2015.
- R. T. Rockafellar. *Convex Analysis*, volume 28 of *Princeton Mathematics Series*. Princeton University Press, Princeton, NJ, 1970.
- Jascha Sohl-Dickstein, Peter Battaglino, and Michael R DeWeese. Minimum probability flow learning. In *Proceedings of the 28th International Conference on International Conference on Machine Learning*, pages 905–912. Omnipress, 2011.
- Jiaming Song, Shengjia Zhao, and Stefano Ermon. A-nice-mc: Adversarial training for mcmc. In *Advances in Neural Information Processing Systems*, pages 5140–5150, 2017.
- Bharath Sriperumbudur, Kenji Fukumizu, Arthur Gretton, Aapo Hyvärinen, and Revant Kumar. Density estimation in infinite dimensional exponential families. *The Journal of Machine Learning Research*, 18(1): 1830–1888, 2017.
- Dougal J Sutherland, Heiko Strathmann, Michael Arbel, and Arthur Gretton. Efficient and principled score estimation with nyström kernel exponential families. *arXiv preprint arXiv:1705.08360*, 2017.
- Tijmen Tieleman. Training restricted Boltzmann machines using approximations to the likelihood gradient. In *Proceedings of the International Conference on Machine Learning*, 2008.
- Tijmen Tieleman and Geoffrey Hinton. Using fast weights to improve persistent contrastive divergence. In *Proceedings of the 26th Annual International Conference on Machine Learning*, pages 1033–1040. ACM, 2009.
- David Vickrey, Cliff Chiung-Yu Lin, and Daphne Koller. Non-local contrastive objectives. In *Proceedings of the International Conference on Machine Learning*, 2010.
- M. J. Wainwright and M. I. Jordan. Graphical models, exponential families, and variational inference. *Foundations and Trends in Machine Learning*, 1(1 – 2):1–305, 2008.
- Ying Nian Wu, Jianwen Xie, Yang Lu, and Song-Chun Zhu. Sparse and deep generalizations of the frame model. *Annals of Mathematical Sciences and Applications*, 3(1):211–254, 2018.

Linfeng Zhang, Weinan E, and Lei Wang. Monge-Ampère flow for generative modeling. *arXiv preprint arXiv:1809.10188*, 2018.

Song Chun Zhu and David Mumford. Grade: Gibbs reaction and diffusion equations. In *Sixth International Conference on Computer Vision (IEEE Cat. No. 98CH36271)*, pages 847–854. IEEE, 1998.

# Appendix

## A Proof of Theorems in Section 3

**Theorem 2 (HMC embeddings as gradient flow)** *For a continuous time with infinitesimal stepsize  $\eta \rightarrow 0$ , the density of the particles  $(x^t, v^t)$ , denoted as  $q_t(x, v)$ , follows Fokker-Planck equation*

$$\frac{\partial q^t(x, v)}{\partial t} = \nabla \cdot (q^t(x, v) G \nabla \mathcal{H}(x, v)), \quad (37)$$

with  $G = \begin{bmatrix} 0 & \mathbf{I} \\ -\mathbf{I} & 0 \end{bmatrix}$ . Then  $q^t(x, v) \rightarrow p(x, v) \propto \exp(-\mathcal{H}(x, v))$  as  $t \rightarrow \infty$ .

**Proof** The first part of the theorem is trivial. When  $\eta \rightarrow 0$ , the HMC follows the dynamical system

$$\left[ \frac{dx}{dt}, \frac{dv}{dt} \right] = [\partial_v \mathcal{H}(x, v), -\partial_x \mathcal{H}(x, v)] = G \nabla \mathcal{H}(x, v).$$

By applying the Fokker-Planck equation, we obtain

$$\frac{\partial q^t(x, v)}{\partial t} = \nabla \cdot (q^t(x, v) G \nabla \mathcal{H}(x, v)). \quad (38)$$

To show that the stationary distribution of such dynamical system converges to  $p(x, v) \propto \exp(-\mathcal{H}(x, v))$ , recall the fact that

$$\nabla \cdot (G \nabla q^t(x, v)) = -\partial_x \partial_v q^t(x, v) + \partial_v \partial_x q^t(x, v) = 0, \quad (39)$$

The Fokker-Planck equation can be rewritten as

$$\frac{\partial q^t(x, v)}{\partial t} = \nabla \cdot (q^t(x, v) G \nabla \mathcal{H}(x, v) + G \nabla q^t(x, v)). \quad (40)$$

Substitute  $p(x, v) \propto \exp(-\mathcal{H}(x, v))$  into (40) and notice

$$\exp(-\mathcal{H}(x, v)) \nabla \mathcal{H}(x, v) + \nabla \exp(-\mathcal{H}(x, v)) = 0,$$

we have  $\partial p(x, v) = 0$ , i.e.,  $p(x, v)$  is the stationary distribution. ■

**Theorem 3 (Density value evaluation)** *If  $(x^0, v^0) \sim q_\theta^0(x, v)$ , after  $T$  vanilla HMC steps (14), we have*

$$q^T(x^T, v^T) = q_\theta^0(x^0, v^0).$$

*For the  $(x^T, v^T)$  from the generalized leapfrog steps (17), we have*

$$q^T(x^T, v^T) = q_\theta^0(x^0, v^0) \prod_{t=1}^T (\Delta_x(x^t) \Delta_v(v^t)),$$

where  $\Delta_x(x^t)$  and  $\Delta_v(v^t)$  are defined in (41).

*For the  $(x^T, \{v^i\}_{i=1}^T)$  from the stochastic Langevin dynamics (20) with  $(x^0, \{\xi^i\}_{i=0}^{T-1}) \sim q_\theta^0(x, \xi) \prod_{i=1}^{T-1} q_{\theta_i}(\xi^i)$ , we have*

$$q^T(x^T, \{v^i\}_{i=1}^T) = q_\theta^0(x^0, \xi^0) \prod_{i=1}^{T-1} q_{\theta_i}(\xi^i).$$

**Proof** The claim can be obtained by simply applying the change-of-variable rule, *i.e.*,

$$q^T(x^T, v^T) = q_\theta^0(x^0, v^0) \prod_{t=1}^T |\det \nabla \mathbf{L}_{f,M}(x^t, v^t)|.$$

The Jacobian of the transformation from  $(x, v)$  to  $(x, v^{-\frac{1}{2}})$  is  $\begin{bmatrix} \mathbf{I} & \mathbf{0} \\ \frac{\eta}{2} \nabla_x^2 f(x) & \mathbf{I} \end{bmatrix}$ , whose determinant is 1.

Similarly, the determinant of the Jacobian of the transform from  $(x, v^{-\frac{1}{2}})$  to  $(x', v')$  is also 1. Therefore,  $|\det(\nabla \mathbf{L}_{f,M}(x^t, v^t))| = 1, \forall i = 1, \dots, T$ , and we prove the first claim.

The second claim can also be obtained in a similar way. By simple algebraic manipulations, we have that the Jacobians of the transformation are all diagonal matrices. Thus,

$$\begin{aligned} \Delta_x(x^t) &= |\det(\text{diag}(\exp(2S_v(\nabla_x f(x^t), x^t))))|, \\ \Delta_v(v^t) &= |\det(\text{diag}(\exp(S_x(v^{\frac{1}{2}}))))|. \end{aligned} \quad (41)$$

Similarly, we calculate the Jacobian for the stochastic Langevin update. Specifically, during the  $t$ -th step, the Jacobian of the transformation from  $(x^{t-1}, \{v^i\}_{i=1}^{t-1}, \xi^{t-1})$  to  $(x^{t-1}, \{v^i\}_{i=1}^{t-1}, v^t)$  is  $\begin{bmatrix} \mathbf{I} & \mathbf{0} & \mathbf{0} \\ \mathbf{0} & \mathbf{I} & \mathbf{0} \\ \frac{\eta}{2} \nabla_x^2 f(x) & \mathbf{0} & \mathbf{I} \end{bmatrix}$ , whose determinant is 1. Similarly, the Jacobian of the transformation from  $(x^{t-1}, \{v^i\}_{i=1}^{t-1}, v^t)$  to  $(x^t, \{v^i\}_{i=1}^{t-1}, v^t)$  is  $\begin{bmatrix} \mathbf{I} & \mathbf{0} & \mathbf{0} \\ \mathbf{0} & \mathbf{I} & \mathbf{0} \\ \mathbf{0} & \mathbf{0} & \mathbf{I} \end{bmatrix}$ , whose determinant is also 1. Therefore  $|\det(\nabla \mathbf{L}_f(x^t, \{v^i\}_{i=1}^t))| = 1$ , which implies

$$q^t(x^t, \{v^i\}_{i=1}^{t-1}, v^t) = q^{t-1}(x^{t-1}, \{v^i\}_{i=1}^{t-1}, \xi^{t-1}) = q^{t-1}(x^{t-1}, \{v^i\}_{i=1}^{t-1}) q_{\theta^{t-1}}(\xi^{t-1}).$$

Apply the same argument for  $\forall t = 1, \dots, T$ , we obtain the third claim. ■

## B Variants of Dynamics Embedding

Besides the vanilla Hamiltonian/Langevin embedding and its generalized version we introduced in the main text, we can also embed alternative dynamics, *i.e.*, deterministic Langevin dynamics and its continuous and generalized version.

### B.1 Deterministic Langevin Embedding

The Hamiltonian dynamics requires an auxiliary variable  $v$  with the same size of the  $x$ , doubling the memory cost. We embed the *deterministic Langevin dynamics* to form  $x' = \mathbf{L}_{f,M}(x)$  as  $x' = x + \eta \nabla_x f(x)$  with  $x^0 \sim q_\theta^0(x)$ . By the change-of-variable rule, we have  $q_{f,M}^T(x^T) = q_\theta^0(x_0) \prod_{t=1}^T \left| \det \frac{\partial x^t}{\partial x^{t-1}} \right|$ . The deterministic Langevin embedding has been exploited in variational auto-encoder (Dai et al., 2018b), in which the variational technique has been applied to bypass the calculation of  $\prod_{t=1}^T \left| \det \frac{\partial x^t}{\partial x^{t-1}} \right|$ .

Plug such parametrization of the dual distribution into (9), we achieve the alternative objective

$$\max_{f \in \mathcal{F}} \min_{\theta, M, \eta} \ell(f; \theta, M, \eta) := \widehat{\mathbb{E}}_{\mathcal{D}}[f] - \mathbb{E}_{x^0 \sim q_\theta^0(x)} \left[ f(x^T) - \log q_\theta^0(x) - \sum_{t=1}^T \log \left| \det \frac{\partial x^t}{\partial x^{t-1}} \right| \right]. \quad (42)$$

For the log-determinant term,  $\log \left| \det \frac{\partial x^t}{\partial x^{t-1}} \right| = \log \left| \det (I + \eta \mathbf{H}^f(x^t)) \right|$ , where  $\mathbf{H}_{i,j}^f = \frac{\partial^2 f(x)}{\partial x_i \partial x_j}$ . Then, the gradient  $\frac{\partial \log |\det(I + \eta \mathbf{H}^f(x^t))|}{\partial f} = \eta \operatorname{tr} \left( (I + \eta \mathbf{H}^f(x_t))^{-1} \frac{\partial \mathbf{H}^f(x^t)}{\partial f} \right)$ . However, the computation of the log-determinant and its derivative w.r.t.  $f$  are expensive. We can apply the polynomial expansion to approximate it.

Denoting  $\delta$  as the bound of the spectrum of  $\mathbf{H}^f(x^t)$  and  $C := \frac{\eta \delta}{1 + \eta \delta} I - \frac{1}{1 + \eta \delta} \mathbf{H}^f(x^t)$ , we have  $\lambda(C) \in (-1, 1)$ . Then,

$$\log |\det (I + \eta \mathbf{H}^f(x^t))| = d \log (1 + \eta \delta) + \operatorname{tr} (\log (I - C)).$$

We can apply Taylor expansion or Chebyshev expansion to approximate the  $\operatorname{tr} (\log (I - C))$ . Specifically, we have

- Stochastic Taylor Expansion (Boutsidis et al., 2017) Recall  $\log (1 - x) = -\sum_{k=1}^{\infty} \frac{x^k}{k}$ , we have the Taylor expansion

$$\operatorname{tr} (\log (I - C)) = -\sum_{i=1}^k \frac{\operatorname{tr} (C^i)}{i}.$$

To avoid the matrix-matrix multiplication, we further approximate the  $\operatorname{tr} (C) = \mathbb{E}_z [z^\top C z]$  with  $z$  as Rademacher random variables, *i.e.*, Bernoulli distribution with  $p = \frac{1}{2}$ .

Particularly, if we set  $i = 1$ , recall the  $\operatorname{tr} (\mathbf{H}^f(x)) = \nabla_x^2 f(x)$ , we can directly calculate without the Hutchinson approximation.

- Stochastic Chebyshev Expansion (Han et al., 2015) We can approximate with Chebyshev polynomial, *i.e.*,

$$\operatorname{tr} (\log (I - C)) = \sum_{i=1}^k c_i \operatorname{tr} (R_i(C)),$$

where  $R(\cdot)$  denotes the Chebyshev polynomial as  $R_i(x) = 2xR_{i-1}(x) - R_{i-2}(x)$  with  $R_1(x) = x$  and  $R_0(x) = 1$ . The  $c_i = \frac{2}{k+1} \sum_{j=0}^k \log(1 - s_j) R_i(s_j)$  if  $i \geq 1$ , otherwise  $c_0 = \frac{1}{n+1} \sum_{j=0}^k \log(1 - s_j)$  where  $s_j = \cos \left( \frac{\pi(k + \frac{1}{2})}{k+1} j \right)$  for  $j = 0, 1, \dots, k$ .

Similarly, we can use the Hutchinson approximation to avoid matrix-matrix multiplication.

## B.2 Continuous-time Langevin Embedding

We discuss several discretized dynamics embedding above. In this section, we take the continuous-time limit  $\eta \rightarrow 0$  in the deterministic Langevin dynamics, *i.e.*,  $\frac{dx}{dt} = \nabla_x f(x)$ . Follow the change-of-variable rule, we obtain

$$\begin{aligned} q(x') &= p(x) \det (I + \eta \mathbf{H}^f(x)) \\ \Rightarrow \log q(x') - \log p(x) &= -\operatorname{tr} \log (I + \eta \mathbf{H}^f(x)) = -\eta \nabla_x^2 f(x) + \mathcal{O}(\eta^2). \end{aligned}$$

As  $\eta \rightarrow 0$ , we have

$$\frac{d \log q(x, t)}{dt} = -\nabla_x^2 f(x). \quad (43)$$

**Remark (connections to Fokker-Planck equation):** Consider the  $\frac{dx}{dt} = \nabla_x f(x)$  as a SDE with zero diffusion term, by Fokker-Planck equation, we obtain the PDE w.r.t.  $q(x, t)$  as

$$\frac{\partial q(x, t)}{\partial t} = -\nabla \cdot (\nabla_x f(x) q(x, t)).$$

Alternatively, we can also derive the (43) from the Fokker-Planck equation by explicitly writing the derivative. Specifically,

$$\begin{aligned}
\frac{dq(x,t)}{dt} &= \frac{\partial q(x,t)}{\partial x} \frac{\partial x}{\partial t} + \frac{\partial q(x,t)}{\partial t} \\
&= \frac{\partial q(x,t)}{\partial x} \nabla_x f(x) - \nabla \cdot (\nabla_x f(x) q(x,t)) \\
&= \frac{\partial q(x,t)}{\partial x} \nabla_x f(x) - \nabla_x^2 f(x) q(x,t) - \nabla_x f(x) \frac{\partial q(x,t)}{\partial t} \\
&= -\nabla_x^2 f(x) q(x,t).
\end{aligned}$$

Therefore, we have

$$\frac{1}{q(x,t)} \frac{dq(x,t)}{dt} = -\nabla_x^2 f(x) \Rightarrow \left[ \frac{d \log q(x,t)}{\frac{dx}{dt}} = -\nabla_x^2 f(x) \right]. \quad (44)$$

Based on (43), we can obtain the samples and its density value by

$$\left[ \log q(x^t) - \log p_\theta^0(x^0) \right] = \int_{t_0}^{t_1} \begin{bmatrix} \nabla_x f(x(t)) \\ -\nabla_x^2 f(x(t)) \end{bmatrix} dt := \mathbf{L}_{f,t_0,t_1}(x). \quad (45)$$

We emphasize that this dynamics is different from the continuous-time flow proposed in Grathwohl et al. (2018), where we have  $\nabla_x^2 f(x)$  in the ODE rather than a trace operator, which requires one more Hutchinson stochastic approximation. We noticed that Zhang et al. (2018) also exploits the Monge-Ampère equation to design the flow-based model for unsupervised learning. However, their learning algorithm is totally different from ours. They use the parameterization as a new flow and fit the model by matching a *separate* distribution; while in our case, the exponential family and flow share the same parameters and match each other automatically.

We can approximate the integral using a numerical quadrature methods. One can approximate the  $\nabla_{(f,t_0,t_1)} \ell(f; t_0, t_1)$  by the derivative through the numerical quadrature. Alternatively, we denote  $g(t) = -\frac{\partial \ell(f, t_0, t_1)}{\partial x(t)}$ , by the adjoint method, the  $\frac{\partial \ell(f, t_0, t_1)}{\partial f}$  is also characterized by ODE

$$\frac{\partial \ell(f, t_0, t_1)}{\partial f} = \int_{t_0}^{t_1} -g(t)^\top \nabla_f \cdot \nabla_x f(x) dt, \quad (46)$$

and can be approximated by numerical quadrature too.

We can combine the discretized and continuous-time Langevin dynamics by simply stacking several layers of  $\mathbf{L}_{f,t_0,t_1}$ .

### B.3 Generalized Continuous-time Langevin Embedding

We generalize the continuous-time Langevin dynamics by introducing more learnable space as

$$\frac{dx}{dt} = h(\xi_f(x)), \quad (47)$$

where  $h$  can be arbitrary smooth function and  $\xi_f(x) = (\nabla_x f(x), f(x), x)$ . We now derive the distributions formed by such flows following the change-of-variable rule, *i.e.*,

$$\begin{aligned}
q(x') &= p(x) \det(I + \eta \nabla_x h(\xi_f(x))) \\
\Rightarrow \log q(x') - \log p(x) &= -\text{tr} \log(I + \eta \nabla_x h(\xi_f(x))) = -\eta \text{tr}(\nabla_x h(\xi_f(x))) + \mathcal{O}(\eta^2).
\end{aligned}$$

As  $\eta \rightarrow 0$ , we have

$$\frac{d \log q(x,t)}{dt} = -\text{tr}(\nabla_x h(\xi_f(x))). \quad (48)$$

Similarly, we can compute the samples and its density value by

$$\left[ \log q(x^t) - \log p_\theta^0(x^0) \right] = \int_{t_0}^{t_1} \begin{bmatrix} h(\xi_f(x)) \\ -\text{tr}(\nabla_x h(\xi_f(x))) \end{bmatrix} dt := \mathbf{L}_{f,t_0,t_1}(x). \quad (49)$$

## C Practical Algorithm

In this section, we discuss several key components in the implementation of the Algorithm 1, including the gradient computation and the parametrization of the initialization  $q_\theta(x, v)$ .

### C.1 Gradient Estimator

The gradient w.r.t.  $f$  is illustrated in (27). The computation of the gradient needs to compute back-propagated through time, therefore, the computational cost is proportional to the number of sampling steps  $T$ .

By Denskin's theorem (Bertsekas, 1995), if the samples  $(x, v)$  from the optimal solution  $p(x, v) \propto \exp(-\mathcal{H}(x, v))$ , the third term in (27) is exactly zero, *i.e.*,

$$\nabla_f \ell(f; \Theta) = \widehat{\mathbb{E}}_{\mathcal{D}} [\nabla_f f(x)] - \mathbb{E}_{(x, v) \sim p(x, v)} [\nabla_f f(x)], \quad (50)$$

whose computational cost is independent to  $T$ .

Recall Theorem 2 that as  $\eta \rightarrow 0$  and  $T \rightarrow \infty$ , the HMC embedding converges to the optimal solution. Therefore, we can approximate the BPTT estimator (27) with the truncated gradient (50). As  $T$  increasing, the corresponding dual sampler approaches the optimal solution, and the truncation bias becomes smaller.

### C.2 Initialization Distribution Parametrization

In our algorithm, the dual distribution are parametrized via dynamics sampling method with an initial distribution  $q_\theta^0(x, v)$ , whose density value is available. There are several possible parametrization:

- **Flow-based model:** The most straightforward parametrization for  $q_\theta^0(x, v)$  is utilizing flow-based model (Rezende and Mohamed, 2015; Dinh et al., 2016; Kingma and Dhariwal, 2018). For simplicity, we can decompose  $q_\theta^0(x, v) = q_{\theta_1}^0(x) q_{\theta_2}^0(v)$  and parametrized both  $q_{\theta_1}^0(x)$  and  $q_{\theta_2}^0(v)$  separately.
- **Variants of deterministic Langevin embedding:** The expression ability of flow-based models is still restricted. We can exploit the deterministic Langevin embedding with separate potential function as the initialization. Specifically, we can also decompose  $q_\theta^0(x, v) = q_{\theta_1}^0(x) q_{\theta_2}^0(v)$ , for the sampler  $x$ , we exploit

$$x^{t+1} = x^t + \epsilon \phi^t(x^t).$$

Although we do not have the explicit  $\log q_{\theta_1}^0(x)$ , we can approximate it via either Taylor expansion or Chebyshev expansion as Section B.1. It should be emphasized that in such parametrization, in each layer we use different  $\phi^t$  for  $t = \{1, \dots, T\}$ , which are all different from  $\nabla_x f(x)$ .

- **Deep latent variable model:** We can also consider the model

$$v \sim q_{\theta_2}^0(v), \quad (51)$$

$$x = \phi_{\theta_1}(v) + \epsilon, \quad \epsilon \sim \mathcal{N}(0, \Sigma), \quad (52)$$

where  $q_{\theta_2}^0(v)$  is some known distribution with  $\theta_2$  as parameter and  $\phi_{\theta_1}$  denotes the neural network with  $\theta_1$  as parameter. Therefore, we have the distribution as

$$q_\theta^0(x, v) = \mathcal{N}(x; \phi_{\theta_1}^0(v), \Sigma) q_{\theta_2}^0(v).$$

For vanilla HMC with leap-frog, the auxiliary variable  $v$  should be the same size as  $x$ . However, for generalized HMC, the dimension of  $v$  can be smaller than that of  $x$ .

- **Nonparametric model:** We can also prefix the  $q^0(x, v) = q^0(x) q^0(v)$  without learning. Specifically, we set  $q^0(x)$  as the empirical  $p_{\mathcal{D}}(x)$  and  $q^0(v) = \mathcal{N}(0, \mathbf{I})$ . Since the initial distribution is fixed, the learning objective (12) reduces to

$$\max_{f \in \mathcal{Q}} \min_{\Theta} \ell(f, \Theta) \propto \widehat{\mathbb{E}}_{\mathcal{D}}[f] - \mathbb{E}_{(x^0, v^0) \sim q^0(x, v)} \left[ f(x^T) - \frac{1}{2} \|v^T\|_2^2 \right]. \quad (53)$$

### C.3 Architecture for Real-world Image Experiments

We demonstrate the architectures of potential function  $f$  and initial Deep LVM in Table 3. A leaky ReLU follows each convolutional/deconvolutional layer in both the discriminator and generator. For the discriminator, we use spectral normalization for all layers in the discriminator. In addition, there is no activation function after the final fully-connected layer. For each deconvolution layer in the generator, we insert a batch normalization layer before passing the output to the leaky ReLU.

Potential function $f(\cdot)$		Initial dual sampler
3x3 conv, 128		fc, $512 \rightarrow 4 \times 4 \times 512$
2x2 avg pool		Reshape to $4 \times 4$ Feature Map
3x3 conv, 256		2x2 Deconv, 256, stride 2
3x3 conv, 256		2x2 Deconv, 128, stride 2
2x2 avg pool		2x2 Deconv, 64, stride 2
3x3 conv, 256		3x3 Deconv, 3, stride 1
3x3 conv, 256		
4x4 avg pool		
fc, $256 \rightarrow 1$		

(a) Potential function  $f(\cdot)$ 
(b) initial dual sampler

Table 3: Our architectures for both potential function  $f(x)$  and initial dual sampler  $p_\theta^0(x, v)$  used in MNIST and CIFAR-10 experiments.

## D More Experiment Results

We illustrated additional generated images by the proposed ADE on MNIST and CIFAR-10 in Figure 4 and Figure 5, respectively.



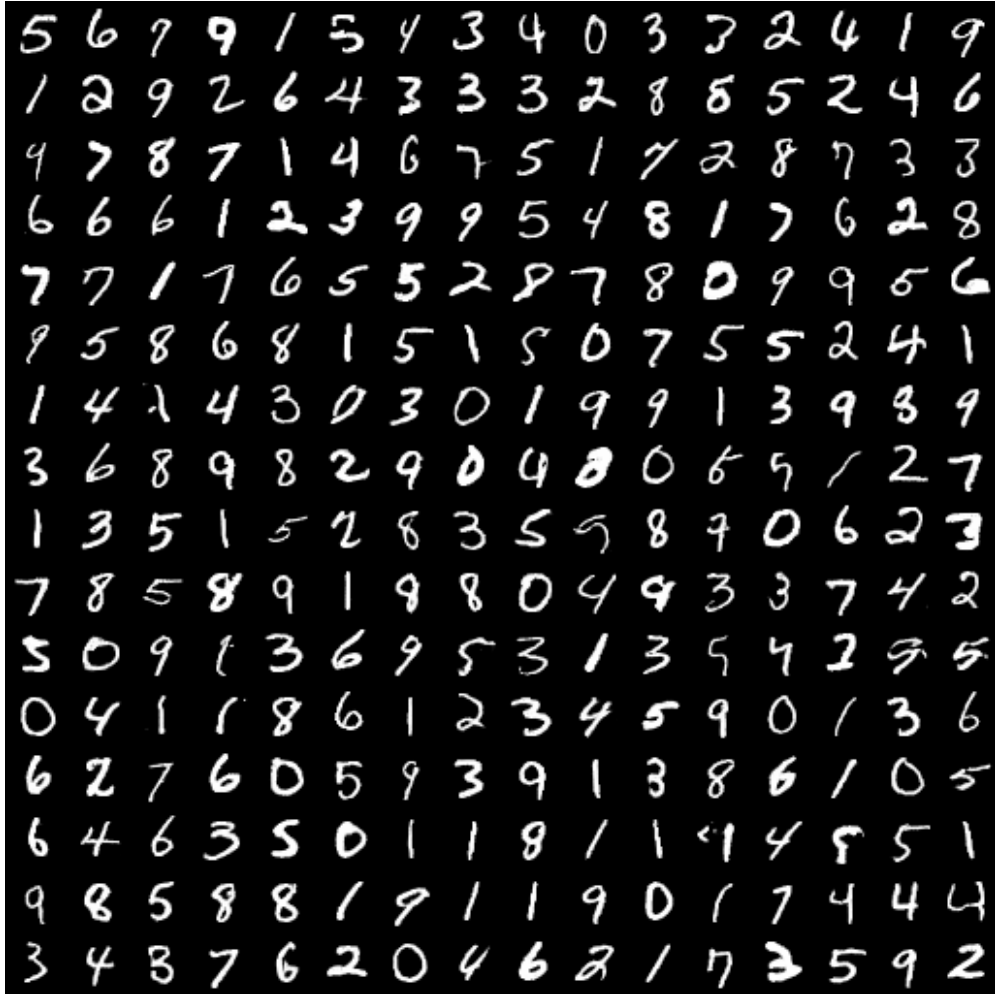


Figure 4: Generated images for MNIST by ADE.



Figure 5: Generated images for CIFAR-10 by ADE.